

# Optimizing the Definition of a Sudden Stratospheric Warming

AMY H. BUTLER

*Cooperative Institute for Research in Environmental Sciences, University of Colorado Boulder,  
and Chemical Sciences Division, National Oceanic and Atmospheric Administration/Earth  
System Research Laboratory, Boulder, Colorado*

EDWIN P. GERBER

*Courant Institute of Mathematical Sciences, New York University,  
New York, New York*

(Manuscript received 27 September 2017, in final form 22 December 2017)

## ABSTRACT

Various criteria exist for determining the occurrence of a major sudden stratospheric warming (SSW), but the most common is based on the reversal of the climatological westerly zonal-mean zonal winds at 60° latitude and 10 hPa in the winter stratosphere. This definition was established at a time when observations of the stratosphere were sparse. Given greater access to data in the satellite era, a systematic analysis of the optimal parameters of latitude, altitude, and threshold for the wind reversal is now possible. Here, the frequency of SSWs, the strength of the wave forcing associated with the events, changes in stratospheric temperature and zonal winds, and surface impacts are examined as a function of the stratospheric wind reversal parameters. The results provide a methodical assessment of how to best define a standard metric for major SSWs. While the continuum nature of stratospheric variability makes it difficult to identify a decisively optimal threshold, there is a relatively narrow envelope of thresholds that work well—and the original focus at 60° latitude and 10 hPa lies within this window.

## 1. Introduction

In the decades following the first observations of a major sudden stratospheric warming (SSW) by Scherhag (1952), various metrics were developed to classify extreme events in the stratosphere (Butler et al. 2015). During an SSW, the winter stratosphere rapidly warms and the climatological westerly polar vortex decelerates, often reversing entirely. Thus the earliest SSW definitions adopted by the World Meteorological Organization (WMO) focused on temperature gradient and zonal wind reversals at the 10-hPa pressure level (~30 km), and poleward of 60° latitude (WMO/IQSY 1964; Quiroz et al. 1975; WMO CAS 1978, p. 36, item 9.4.4; McInturff 1978; Labitzke 1981). The initial focus on 10 hPa and

60°N arose from careful synoptic analysis of where the greatest changes were being observed during these events (WMO/IQSY 1964). It was also likely informed by the availability of data; most of the earliest observations were taken by radiosondes and rocketsondes equatorward of 60°N over Northern Hemisphere (NH) midlatitude land regions (Oort and Liu 1993). Today the most commonly used definition for SSWs still relies on the zonal-mean zonal wind reversal at 60° latitude and 10 hPa (Charlton and Polvani 2007).

Recent work has shown, however, that the classification of major SSWs by this simple zonal wind definition is sensitive to the choice of latitude, pressure level, and threshold used to detect the events (Butler et al. 2015; Palmeiro et al. 2015). Various other techniques, including annular modes (Baldwin 2001; Baldwin and Thompson 2009; Gerber et al. 2010), geometric vortex diagnostics (Waugh and Randel 1999; Hannachi et al. 2011; Mitchell et al. 2011; Seviour et al. 2013), deceleration-based measures (Kim et al. 2017), temperature changes (Blume et al. 2012; Maury et al. 2016), and empirical orthogonal

---

Supplemental information related to this paper is available at the Journals Online website: <http://dx.doi.org/10.1175/JCLI-D-17-0648.s1>.

---

Corresponding author: Amy Butler, amy.butler@noaa.gov

functions (EOFs) (Hitchcock et al. 2013) have also been used to detect extreme polar vortex events. These too ultimately rely on arbitrary thresholds, are sensitive to the parameters chosen, and can be more computationally intensive.

Given the sizable increase in measurements of the middle atmosphere since the satellite-era began, we conduct a systematic evaluation of where a zonal wind reversal should be defined in order to “optimize” the classification of major SSWs. The detection algorithm should, first and foremost, isolate events that are 1) sudden, involving a rapid deceleration of the stratospheric polar vortex, and 2) warming, with a large-amplitude temperature increase. Ideally, the definition will also capture events with significant two-way coupling between the troposphere and stratosphere, maximizing 3) the upward wave propagation into the stratosphere prior to events and 4) the downward coupling of the zonal mean circulation to the surface after events. After presenting our methodology in section 2, we consider how the frequency of events changes in relation to pressure level, latitude, and threshold of the zonal wind deceleration and show where criteria 1–4 above are optimized in relation to these parameters in section 3. Our conclusions are presented in section 4.

## 2. Methodology

We use daily-mean output of JRA-55 from 1958 to 2016 (Ebita et al. 2011), but the results are robust to the choice of reanalysis. Daily anomalies are calculated relative to a smooth annual cycle, computed by averaging each calendar day over the entire period, and then filtering in Fourier space by retaining only the first four harmonics. For the Arctic Oscillation (AO) index, we use daily historical values provided by the National Centers for Environmental Prediction (NCEP) Climate Prediction Center (CPC), which are based on EOF analysis of the 1000-hPa geopotential height anomalies from the NCEP–NCAR reanalysis data and standardized by the December–March (DJFM) daily values.

A commonly used definition for major midwinter SSWs is a reversal of the zonal-mean zonal winds at 60°N and 10 hPa during the months of November–March (Charlton and Polvani 2007, hereafter CP07). CP07 require that reversals be separated by at least 20 consecutive days of westerlies to ensure events are independent, and that westerlies must return for at least 10 consecutive days prior to 30 April to avoid including final warmings. Disadvantages of this definition are that, by construction, it does not detect final warmings, and the 30 April requirement is an arbitrary cutoff. We address these with minor changes to the CP07 method.

We extend the analysis from 1 July to 30 June of the following year, and first detect the start and end of the vortex for each year. The start occurs when westerlies persist for at least 10 consecutive days. The end of the vortex, or final warming (FW), occurs on the last date when the winds reverse and do not return to westerly for more than 10 consecutive days. The FWs at 60°N and 10 hPa detected with this method agree reasonably well with previously published FW dates, such as from Hu et al. (2014) (see Table S1 in the supplemental material), while maintaining consistency with the major SSW definition.

SSWs are then detected by reversals during this extended winter season, but with a more stringent requirement that zonal winds must return to westerlies for 30 consecutive days between events, including from the final warming. A 20-day separation, however, does not significantly change our results. Table 1 compares our SSW dates based on zonal wind reversal at 60° latitude and 10 hPa with CP07. Only three events, all in March, are classified as midwinter SSWs by CP07 but not by our method. Two of these dates are not separated from earlier SSW dates by at least 30 consecutive days of westerlies; the other (14 March 1988) does not return to westerlies for at least 30 consecutive days before the final warming (see Fig. S1 in the supplemental material).

Using these separation and final warming criteria, we examine how the dates and synoptic properties of SSWs vary with the latitude and level at which the zonal wind is measured, and with the threshold of deceleration. Here, the “threshold” sets the magnitude to which the vortex winds must decelerate to count as a major event. It has traditionally been defined at  $0 \text{ m s}^{-1}$  because planetary waves cannot propagate into easterly flow (Charney and Drazin 1961). For event separation, with negative thresholds ( $u_c \leq 0 \text{ m s}^{-1}$ ) the winds must return to westerly ( $u > 0 \text{ m s}^{-1}$ ) for at least 30 consecutive days, whereas with positive thresholds ( $u_c > 0 \text{ m s}^{-1}$ ) the winds must exceed  $u_c$  for at least 30 consecutive days after the event.

The mean of each synoptic property in section 3 is found by averaging over all events determined at a given location and threshold. Significance testing is performed via Monte Carlo sampling, in which we repeatedly sample the same day and month of events for a particular set of parameters but randomize the years 500 times. We then determine if the difference in means between the two distributions (assuming unequal variances) exceeds the 95% Student’s  $t$  test. In most cases, the signals are significantly different everywhere. If fewer than two SSWs per decade (i.e., fewer than 12 SSWs from 1958 to 2016) are detected at a given location, the metric is assigned a missing value.

TABLE 1. Major SSWs in the Northern Hemisphere defined by reversals of the zonal wind at 60°N and 10 hPa, for (left) this study and (right) CP07. The last row shows the total number of SSWs.

Major SSWs: This study	Major SSWs: CP07
30 Jan 1958	30 Jan 1958
17 Jan 1960	17 Jan 1960
30 Jan 1963	30 Jan 1963
18 Dec 1965	18 Dec 1965
23 Feb 1966	23 Feb 1966
7 Jan 1968	7 Jan 1968
29 Nov 1968	29 Nov 1968
2 Jan 1970	2 Jan 1970
18 Jan 1971	18 Jan 1971
20 Mar 1971	20 Mar 1971
31 Jan 1973	31 Jan 1973
9 Jan 1977	9 Jan 1977
22 Feb 1979	22 Feb 1979
29 Feb 1980	29 Feb 1980
6 Feb 1981	6 Feb 1981
—	4 Mar 1981
4 Dec 1981	4 Dec 1981
24 Feb 1984	24 Feb 1984
1 Jan 1985	1 Jan 1985
23 Jan 1987	23 Jan 1987
8 Dec 1987	8 Dec 1987
—	14 Mar 1988
21 Feb 1989	21 Feb 1989
15 Dec 1998	15 Dec 1998
26 Feb 1999	26 Feb 1999
20 Mar 2000	20 Mar 2000
11 Feb 2001	11 Feb 2001
31 Dec 2001	31 Dec 2001
18 Jan 2003	18 Jan 2003
5 Jan 2004	5 Jan 2004
21 Jan 2006	21 Jan 2006
24 Feb 2007	24 Feb 2007
22 Feb 2008	22 Feb 2008
24 Jan 2009	24 Jan 2009
9 Feb 2010	9 Feb 2010
—	24 Mar 2010
7 Jan 2013	7 Jan 2013
34	37

### 3. Optimizing the SSW definition

CP07 and Charlton et al. (2007) propose several key metrics for evaluating major SSWs in model simulations (cf. Table 3 in CP07). Here, we consider similar properties, but apply them to zonal wind decelerations everywhere between 50 and 1 hPa, 50°–80°N, and for thresholds from  $-10$  to  $10 \text{ m s}^{-1}$ .

The frequency of SSW events is quite sensitive to where the zonal wind deceleration is defined (Fig. 1; see also Butler et al. 2015). At levels below  $\sim 10$  hPa, the number of zonal wind reversals per decade increases primarily with latitude; at levels above 10 hPa, the frequency is primarily a function of height (Fig. 1a). Note that regions that have similar SSW frequency are not

necessarily detecting the same events. Figure 1c shows the percent match<sup>1</sup> of events within  $\pm 10$  days of CP07 SSW events (i.e., reversals at 10 hPa and 60°N). Zonal wind reversals along the edge of the polar vortex detect greater than 50% of the same events (solid black contour), although similarities greater than 80% are uncommon.

At 10 hPa, the frequency of SSW events decreases if the threshold value is more negative, particularly equatorward of 65°N (Fig. 1b). While more events are detected as the critical threshold is relaxed to more positive values, these events also have weaker dynamic impacts overall (Figs. 2 and 3). The agreement of dates with those at  $0 \text{ m s}^{-1}$  and 10 hPa and 60°N is greater than 50% for a broad range of different thresholds; in particular, as the required threshold becomes more negative, one needs to use decelerations at more poleward locations to detect the same events.

Figure 2 shows how two fundamental synoptic characteristics of SSWs, the suddenness of the vortex breakdown and the magnitude of the temperature increase, vary depending on the location and threshold of the deceleration. “Suddenness” is characterized by the change in the 60°–80°N zonal-mean zonal wind, mass-weighted and vertically averaged from 50 to 1 hPa, computed from the mean of days 0–5 after the event minus days 5–15 prior to each event (Figs. 2a,b). While the vortex must decelerate in all cases to trigger an event, larger values here indicate that the deceleration was more rapid. For example, at 60°N and 10 hPa (Fig. 2a, black dot), the value is  $-12.2 \text{ m s}^{-1}$ : this indicates that, for events defined by a reversal at this location (as in CP07), the entire vortex abruptly slows by  $\sim 12 \text{ m s}^{-1}$  in approximately 10 days. (Note that the winds at a particular location may decelerate far more than the latitudinally and vertically averaged vortex; e.g., the net change in zonal wind at 60°N and 10 hPa is approximately  $-30 \text{ m s}^{-1}$  for reversals occurring there.) If one defines events by a reversal at 70°N and 5 hPa, the average deceleration is weaker, approximately  $-10.6 \text{ m s}^{-1}$ . Overall, we find that the most abrupt events are found when the zonal wind reverses near the climatological maximum of the polar jet in the midstratosphere, from 30 to 5 hPa as one moves from  $\sim 60^\circ$  to  $72^\circ\text{N}$ . Figure 2b shows that if we fix the pressure level at which events are defined at 10 hPa, requiring a stronger threshold (i.e., less

<sup>1</sup> Percent match is calculated here as  $P = A/N \times 100$ , where  $A$  is the number of same events detected at both 10 hPa and 60°N and a particular location, and  $N = A + B + C$ , where  $B$  is the number of events detected at 10 hPa and 60°N but not the other location, and  $C$  is the number of events detected at the particular location but not at 10 hPa and 60°N.

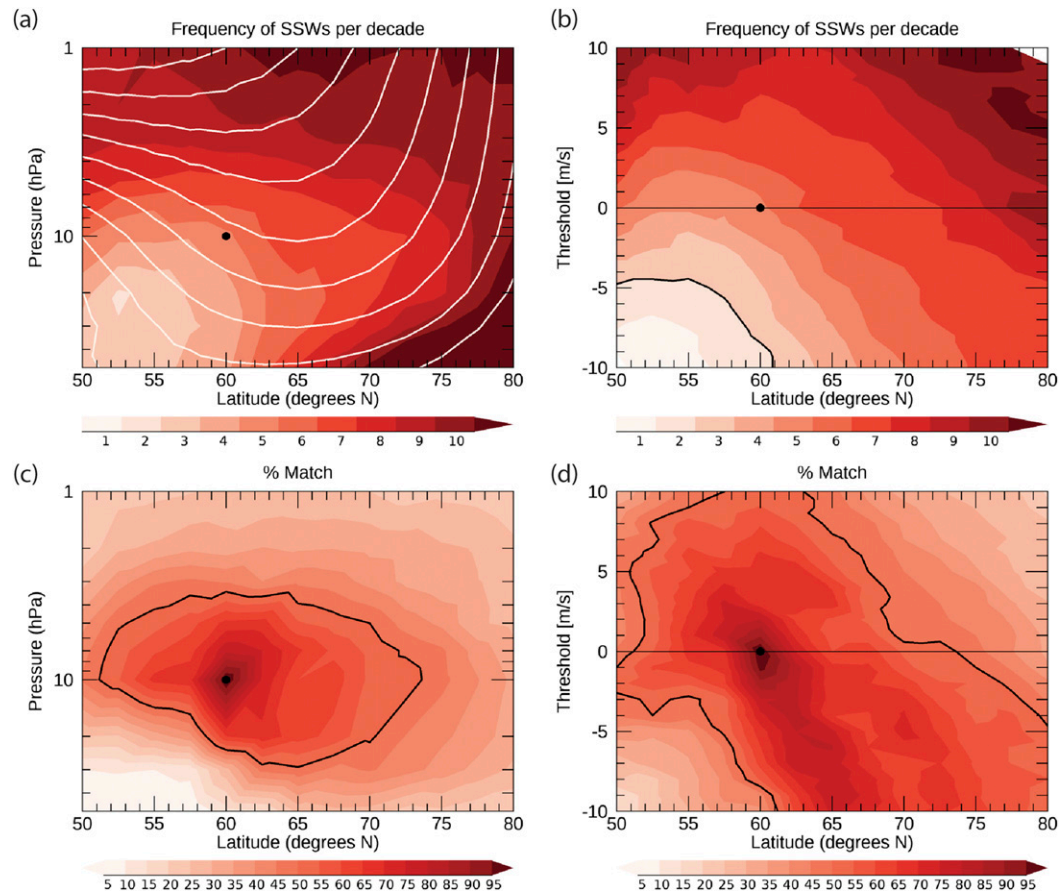


FIG. 1. (a),(b) The frequency or number of SSWs per decade and (c),(d) the percent match of SSW dates at a given location with SSW dates at 60°N, 10 hPa, and a 0 m s<sup>-1</sup> threshold. Thin white contours in (a) show the mean DJFM zonal winds at 3 m s<sup>-1</sup> intervals, with the highest contour near 50°–60°N at 1 hPa equal to 39 m s<sup>-1</sup>. The black contour in (b) indicates where there are fewer than two SSWs per decade; black contours in (c) and (d) indicate where date agreement is higher than 50%.

than  $-2 \text{ m s}^{-1}$ ) selects events with greater deceleration or suddenness. This is partly by construction; a negative threshold will capture fewer, stronger events.

The “warming” metric (Figs. 2c,d) is defined as the polar cap (50°–90°N) temperature anomaly, mass-weighted and vertically averaged from 50 to 1 hPa, for the mean from day  $-5$  to  $+5$  around each event. It is maximized for zonal wind reversals that occur on the equatorward edge of the polar vortex (50°–65°N), from 20 to 5 hPa. As before, requiring a more negative threshold at 10 hPa (Fig. 2d) selects events with larger temperature increases. Note, however, that for events at 60°N with thresholds near from  $+1$  to  $3 \text{ m s}^{-1}$ , both the suddenness and the temperature increase have magnitudes similar to those of events with thresholds from 0 to  $-3 \text{ m s}^{-1}$ . This similarity suggests that wind decelerations that nearly reach  $0 \text{ m s}^{-1}$ , but do not actually reverse the polar vortex, are still associated with substantial dynamic changes in the stratosphere.

Figure 3 considers two additional desirable properties of major SSWs: upward and downward coupling between the troposphere and the stratosphere. Upward wave propagation from the troposphere is represented by the 45°–75°N eddy heat flux ( $v'T'$ ) anomalies at 100 hPa, averaged from days  $-20$  to 0 of each event (Fig. 3a). Reversals occurring equatorward of 65°N and at levels below 10 hPa are associated with stronger poleward (positive) eddy heat flux anomalies prior to the event, indicating that stronger wave driving is necessary to reverse the zonal wind here. Note that there are also fewer reversals that occur here (Fig. 1). Stronger heat flux anomalies are also associated with decelerations below the  $0 \text{ m s}^{-1}$  threshold at 10 hPa (Fig. 3b).

The strength of the stratospheric coupling to the surface is characterized by the mean Arctic Oscillation index for days 0–60 after events (Figs. 3c,d). The AO is the dominant mode of climate variability in the NH

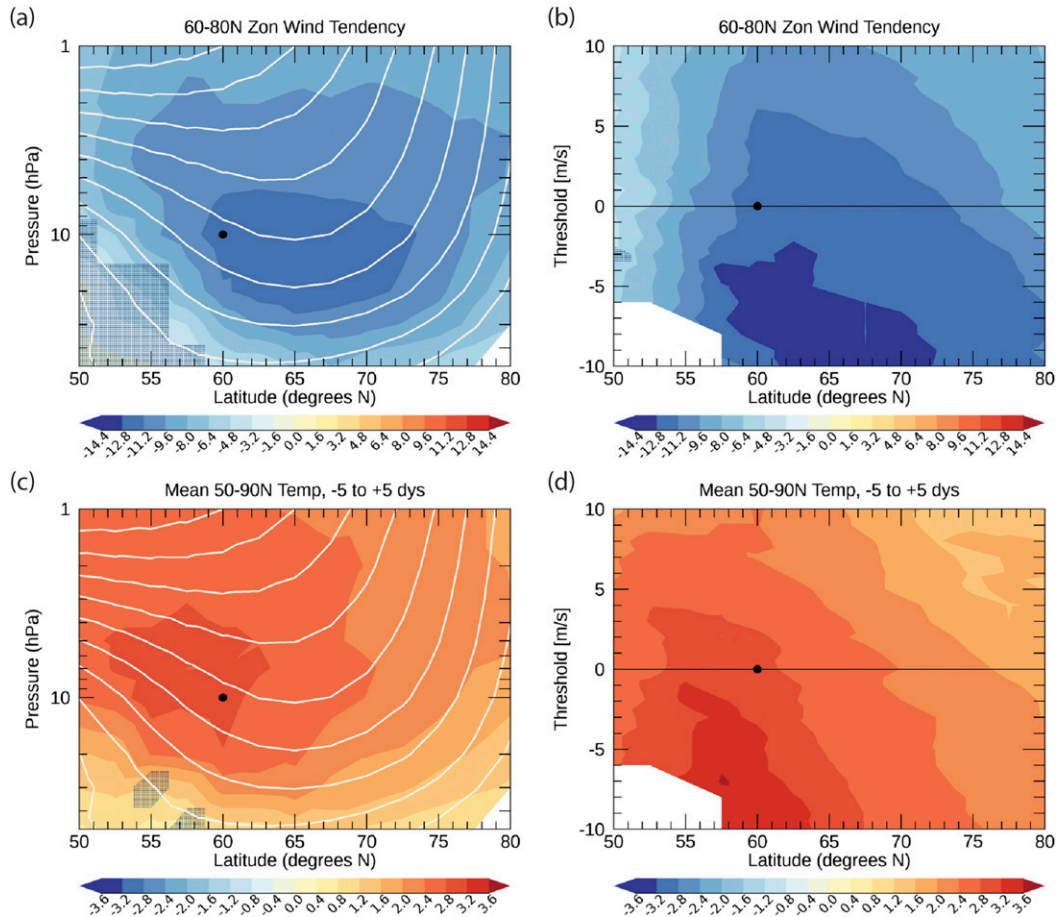


FIG. 2. (a),(b) The mean zonal wind change ( $\text{m s}^{-1}$ ) averaged from  $60^{\circ}$ – $80^{\circ}\text{N}$  and 50–1 hPa for days 0–5 after each reversal minus days 5–15 prior to each reversal, and (c),(d) the mean temperature anomaly (K) averaged from  $50^{\circ}$  to  $90^{\circ}\text{N}$  and 50 to 1 hPa for days –5 to +5 of each reversal, as a function of latitude and (a), (c) pressure level (with a threshold of  $0 \text{ m s}^{-1}$ ) and (b),(d) threshold (at 10 hPa). Thin white contours in (a) and (c) are as in Fig. 1. Stippling indicates where values are *not* significant based on a 95% Student’s *t* test (see details in section 2).

midlatitudes; a weakening of the polar vortex is associated with the negative phase of the AO (i.e., an equatorward shift of the tropospheric storm track). It is clear that reversals in the lower stratosphere between  $\sim 60^{\circ}$  and  $70^{\circ}\text{N}$  result in the largest impacts on the AO (Fig. 3c), in agreement with previous studies (Gerber et al. 2009; Hitchcock and Simpson 2014; Maycock and Hitchcock 2015; Karpechko et al. 2017). Similar results are found for a metric based on Eurasian surface temperature anomalies (not shown). For decelerations at 10 hPa (Fig. 3d), AO impacts are not strongly dependent on threshold, although the largest changes occur for negative thresholds between  $\sim 62^{\circ}$  and  $72^{\circ}\text{N}$ . Comparing the top and bottom rows of Fig. 3, it is seen that wind decelerations with the strongest upward wave driving are not always associated with the strongest influence on the surface.

#### 4. Discussion and conclusions

To summarize these findings, we create a qualitative “score” ranging from 0 to 1 for each of the four key SSW properties (Figs. 2 and 3) by dividing the value of each property at a particular location/threshold by the maximum value observed over all locations/thresholds. A score of 1 then implies the optimal location for a given property. Figure 4 shows the average scores, giving equal weight to each property. While it is somewhat arbitrary to equally weight each property, the scores are not heavily dominated by any one metric. We find that the key properties for SSWs are maximized (average scores  $>0.8$ ) for reversals between  $55^{\circ}$  and  $70^{\circ}\text{N}$  (slightly equatorward of the polar vortex climatological maximum) in the midstratosphere from 30 to 5 hPa (Fig. 4a), and for decelerations near or below  $0 \text{ m s}^{-1}$  (Fig. 4b).

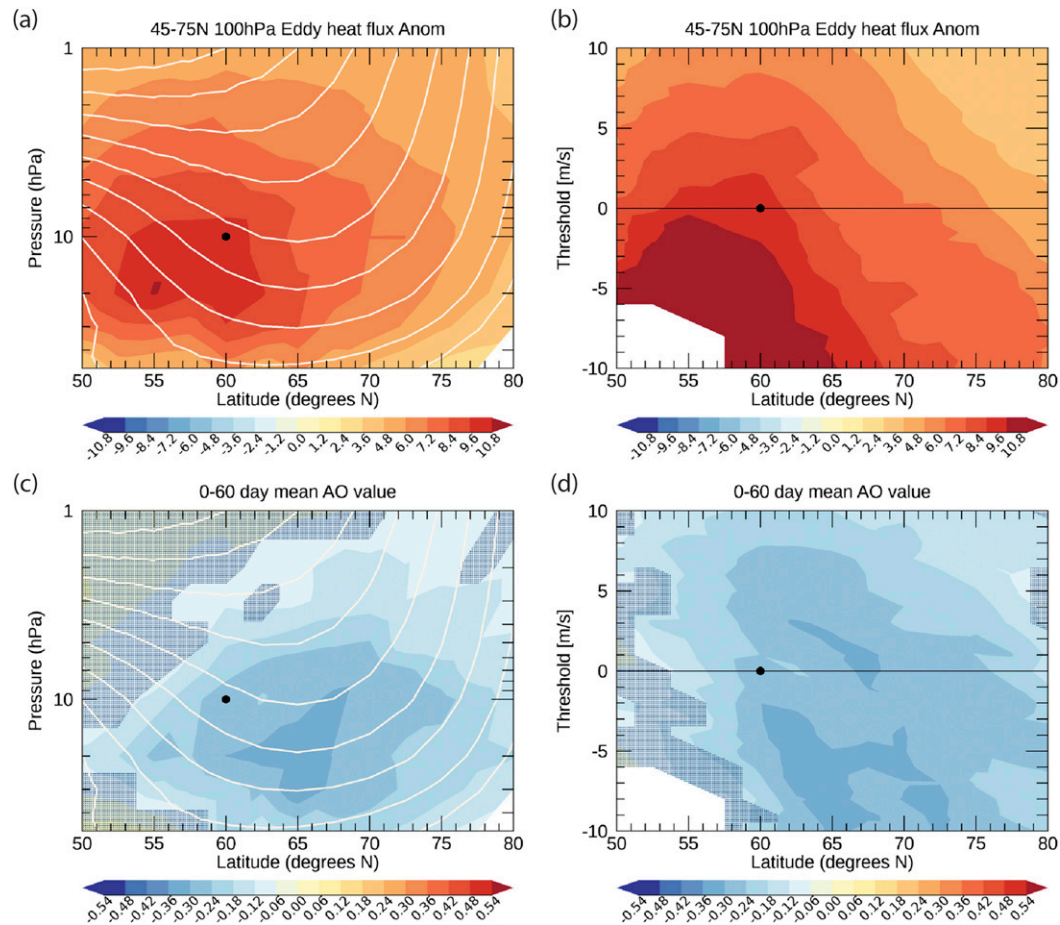


FIG. 3. (a),(b) The mean eddy heat flux anomaly ( $\text{K m s}^{-1}$ ) at 100 hPa and  $45^{\circ}$ – $75^{\circ}$ N for days 20–0 prior to each reversal, and (c),(d) the mean daily Arctic Oscillation index (standardized by the DJFM mean) for days 0–60 after each reversal, as a function of latitude and (a),(c) pressure level (with a threshold of  $0 \text{ m s}^{-1}$ ) and (b),(d) threshold (at 10 hPa). Thin white contours in (a) and (c) are as in Fig. 1. Stippling indicates where values are *not* significant based on a 95% Student's *t* test (see details in section 2).

Removing one of these metrics (or modifying their details) does not qualitatively change this result, although the AO metric tends to depress the scores for events characterized at upper levels.

There is a fairly narrow range of pressure levels, latitudes, and thresholds where features relevant to major SSWs are maximized, and for which there are still a reasonable number of events. Zonal wind reversals at 10 hPa and  $60^{\circ}$ N fall within this region, indicating that the historically used definition does detect SSWs with a strong dynamic response in the stratosphere and strong coupling to the troposphere; this is a testament to the synoptic intuition of meteorologists in the presatellite era. Our results also suggest that while zonal wind decelerations near  $0 \text{ m s}^{-1}$  have similar impacts to true wind reversals, there is a decline in stratospheric and tropospheric impacts as the threshold is relaxed to more positive values.

The optimization could be extended to cover more parameters (e.g., the separation criteria) and metrics (e.g., the surface temperature response), but sampling uncertainty associated with the finite reanalysis record and the continuum nature of stratospheric variability means that defining SSWs will always involve some degree of subjectivity (e.g., Coughlin and Gray 2009). Further analysis is also needed to determine how these results apply to model simulations with mean state biases (e.g., Kim et al. 2017).

There are recent and ongoing efforts to reevaluate and improve the standard definition for SSWs as defined by the WMO (Butler et al. 2014; Butler et al. 2015). While our analysis lends evidence that major changes to the current definition are unwarranted, there are still potential avenues for improvement. These include clarity of the separation criteria and the inclusion of

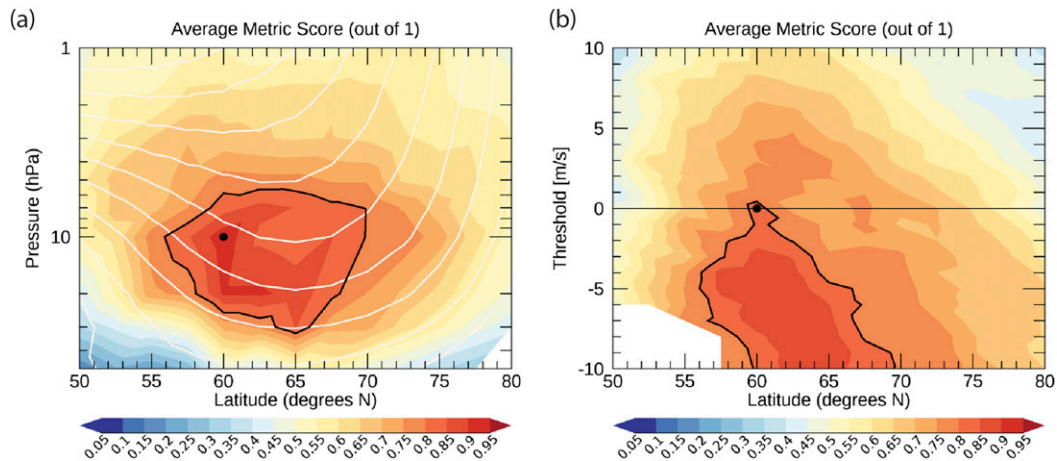


FIG. 4. The average of all the metric scores, defined as the metric at each location divided by the maximum metric, as a function of latitude and (a) pressure level (with a threshold of  $0 \text{ m s}^{-1}$ ) and (b) threshold (at 10 hPa). Thin white contours in (a) and (c) are as in Fig. 1. Solid black line indicates where the metric score exceeds 0.8.

minor and final warmings consistent with the major warming definition.

**Acknowledgments.** We thank three anonymous reviewers for their feedback on an earlier draft of the manuscript. EPG was supported by the U.S. National Science Foundation (AGS-1546585).

#### REFERENCES

- Baldwin, M. P., 2001: Annular modes in global daily surface pressure. *Geophys. Res. Lett.*, **28**, 4115–4118, <https://doi.org/10.1029/2001GL013564>.
- , and D. W. J. Thompson, 2009: A critical comparison of stratosphere–troposphere coupling indices. *Quart. J. Roy. Meteor. Soc.*, **135**, 1661–1672, <https://doi.org/10.1002/qj.479>.
- Blume, C., K. Matthes, and I. Horenko, 2012: Supervised learning approaches to classify sudden stratospheric warming events. *J. Atmos. Sci.*, **69**, 1824–1840, <https://doi.org/10.1175/JAS-D-11-0194.1>.
- Butler, A. H., E. P. Gerber, D. Mitchell, and W. J. M. Seviour, 2014: New efforts in developing a standard definition for sudden stratospheric warmings. SPARC Newsletter, No. 43, ETH Zurich, Zurich, Switzerland, 23–24, <http://www.sparc-climate.org/publications/newsletter/>.
- , D. J. Seidel, S. C. Hardiman, N. Butchart, T. Birner, and A. Match, 2015: Defining sudden stratospheric warmings. *Bull. Amer. Meteor. Soc.*, **96**, 1913–1928, <https://doi.org/10.1175/BAMS-D-13-00173.1>.
- Charlton, A. J., and L. M. Polvani, 2007: A new look at stratospheric sudden warmings. Part I: Climatology and modeling benchmarks. *J. Climate*, **20**, 449–469, <https://doi.org/10.1175/JCLI3996.1>.
- , and Coauthors, 2007: A new look at stratospheric sudden warmings. Part II: Evaluation of numerical model simulations. *J. Climate*, **20**, 470–488, <https://doi.org/10.1175/JCLI3994.1>.
- Charney, J. G., and P. G. Drazin, 1961: Propagation of planetary-scale disturbances from the lower into the upper atmosphere. *J. Geophys. Res.*, **66**, 83–109, <https://doi.org/10.1029/JZ066i001p00083>.
- Coughlin, K., and L. J. Gray, 2009: A continuum of sudden stratospheric warmings. *J. Atmos. Sci.*, **66**, 531–540, <https://doi.org/10.1175/2008JAS2792.1>.
- Ebita, A., and Coauthors, 2011: The Japanese 55-year Reanalysis “JRA-55”: An interim report. *Sci. Online Lett. Atmos.*, **7**, 149–152, <https://doi.org/10.2151/sola.2011-038>.
- Gerber, E. P., C. Orbe, and L. M. Polvani, 2009: Stratospheric influence on the tropospheric circulation revealed by idealized ensemble forecasts. *Geophys. Res. Lett.*, **36**, L24801, <https://doi.org/10.1029/2009GL040913>.
- , and Coauthors, 2010: Stratosphere–troposphere coupling and annular mode variability in chemistry–climate models. *J. Geophys. Res.*, **115**, D00M06, <https://doi.org/10.1029/2009JD013770>.
- Hannachi, A., D. Mitchell, L. Gray, and A. Charlton-Perez, 2011: On the use of geometric moments to examine the continuum of sudden stratospheric warmings. *J. Atmos. Sci.*, **68**, 657–674, <https://doi.org/10.1175/2010JAS3585.1>.
- Hitchcock, P., and I. R. Simpson, 2014: The downward influence of stratospheric sudden warmings. *J. Atmos. Sci.*, **71**, 3856–3876, <https://doi.org/10.1175/JAS-D-14-0012.1>.
- , T. G. Shepherd, and G. L. Manney, 2013: Statistical characterization of Arctic polar-night jet oscillation events. *J. Climate*, **26**, 2096–2116, <https://doi.org/10.1175/JCLI-D-12-00202.1>.
- Hu, J., R. Ren, and H. Xu, 2014: Occurrence of winter stratospheric sudden warming events and the seasonal timing of spring stratospheric final warming. *J. Atmos. Sci.*, **71**, 2319–2334, <https://doi.org/10.1175/JAS-D-13-0349.1>.
- Karpechko, A. Y., P. Hitchcock, D. H. W. Peters, and A. Schneidereit, 2017: Predictability of downward propagation of major sudden stratospheric warmings. *Quart. J. Roy. Meteor. Soc.*, **143**, 1459–1470, <https://doi.org/10.1002/qj.3017>.
- Kim, J., S.-W. Son, E. P. Gerber, and H.-S. Park, 2017: Defining sudden stratospheric warming in climate models: Accounting for biases in model climatologies. *J. Climate*, **30**, 5529–5546, <https://doi.org/10.1175/JCLI-D-16-0465.1>.
- Labitzke, K., 1981: Stratospheric–mesospheric midwinter disturbances—A summary of observed characteristics. *J. Geophys. Res.*, **86**, 9665–9678, <https://doi.org/10.1029/JC086iC10p09665>.
- Maury, P., C. Claud, E. Manzini, A. Hauchecorne, and P. Keckhut, 2016: Characteristics of stratospheric warming events during

- northern winter. *J. Geophys. Res. Atmos.*, **121**, 5368–5380, <https://doi.org/10.1002/2015JD024226>.
- Maycock, A. C., and P. Hitchcock, 2015: Do split and displacement sudden stratospheric warmings have different annular mode signatures? *Geophys. Res. Lett.*, **42**, 10 943–10 951, <https://doi.org/10.1002/2015GL066754>.
- McInturff, R. M., Ed., 1978: Stratospheric warmings: Synoptic, dynamic and general-circulation aspects. Tech. Rep. NASA-RP-1017, 166 pp., <https://ntrs.nasa.gov/archive/nasa/casi.ntrs.nasa.gov/19780010687.pdf>.
- Mitchell, D. M., L. J. Gray, and J. Charlton-Perez, 2011: The structure and evolution of the stratospheric vortex in response to natural forcings. *J. Geophys. Res.*, **116**, D15110, <https://doi.org/10.1029/2011JD015788>.
- Oort, A. H., and H. Liu, 1993: Upper-air temperature trends over the globe, 1958–1989. *J. Climate*, **6**, 292–307, [https://doi.org/10.1175/1520-0442\(1993\)006<0292:UATTOT>2.0.CO;2](https://doi.org/10.1175/1520-0442(1993)006<0292:UATTOT>2.0.CO;2).
- Palmeiro, F. M., D. Barriopedro, R. García-Herrera, and N. Calvo, 2015: Comparing sudden stratospheric warming definitions in reanalysis data. *J. Climate*, **28**, 6823–6840, <https://doi.org/10.1175/JCLI-D-15-0004.1>.
- Quiroz, R. S., A. J. Miller, and R. M. Nagatani, 1975: A comparison of observed and simulated properties of sudden stratospheric warmings. *J. Atmos. Sci.*, **32**, 1723–1736, [https://doi.org/10.1175/1520-0469\(1975\)032<1723:ACOOAS>2.0.CO;2](https://doi.org/10.1175/1520-0469(1975)032<1723:ACOOAS>2.0.CO;2).
- Scherhag, R., 1952: Die explosionsartigen Stratosphärenwärmungen des Spätwinters 1952. *Ber. Det. Wetterdienstes*, **38**, 51–63.
- Seviour, W. J. M., D. M. Mitchell, and L. J. Gray, 2013: A practical method to identify displaced and split stratospheric polar vortex events. *Geophys. Res. Lett.*, **40**, 5268–5273, <https://doi.org/10.1002/grl.50927>.
- Waugh, D. W., and W. J. Randel, 1999: Climatology of Arctic and Antarctic polar vortices using elliptical diagnostics. *J. Atmos. Sci.*, **56**, 1594–1613, [https://doi.org/10.1175/1520-0469\(1999\)056<1594:COAAAP>2.0.CO;2](https://doi.org/10.1175/1520-0469(1999)056<1594:COAAAP>2.0.CO;2).
- WMO CAS, 1978: WMO Commission for Atmospheric Sciences: Abridged Final Report of the Seventh Session, Manila, 27 February–10 March 1978. WMO-No. 509, 113 pp., [http://library.wmo.int/pmb\\_ged/wmo\\_509\\_en.pdf](http://library.wmo.int/pmb_ged/wmo_509_en.pdf).
- WMO/IQSY, 1964: International Years of the Quiet Sun (IQSY) 1964–65. Alert messages with special references to stratwarms. WMO/IQSY Rep. 6, 19 pp.